

Cite this: DOI: 10.1039/c0xx00000x

www.rsc.org/xxxxxx

ARTICLE TYPE

Flying-seed-like liquid crystals **4**[†]: a novel series of bulky substituents inducing mesomorphism instead of using long alkyl chains

Miho Yoshioka,^a Kazuchika Ohta^{*a} and Mikio Yasutake^b

Received (in XXX, XXX) Xth XXXXXXXXXX 20XX, Accepted Xth XXXXXXXXXX 20XX

DOI: 10.1039/b000000x

We have synthesized a novel series of flying-seed-like derivatives (**3a-g**) based on phthalocyaninato copper(II) (abbreviated as PcCu) substituted by bulky groups {PhO (**a**), (*o*-C₁)PhO (**b**), (*m*-C₁)PhO (**c**), (*p*-C₁)PhO (**d**), [*m,p*-(C₁)₂]PhO (**e**), [*m,m'*-(C₁)₂]PhO (**f**), and [*m,p,m'*-(C₁)₃]PhO (**g**)} instead of using long alkyl chains, in order to investigate their mesomorphism. Their phase transition behaviour and the mesophase structures have been established by using a polarizing optical microscope, a differential scanning calorimeter, a thermogravimetry analyser and a temperature-dependent small angle X-ray diffractometer. As a result, (PhO)₈PcCu (**3a**) and [(*p*-C₁)PhO]₈PcCu (**3d**) show no mesophase, whereas [(*m*-C₁)PhO]₈PcCu (**3c**), {[*m,p*-(C₁)₂]PhO}₈PcCu (**3e**), {[*m,m'*-(C₁)₂]PhO}₈PcCu (**3f**), and {[*m,p,m'*-(C₁)₃]PhO}₈PcCu (**3g**) show various kinds of columnar mesophases of Col_{ro}(P2₁/a), Col_{ro}(P2₁/a), Col_{ro}(C2/m) and Col_{tet.o}, respectively; [(*o*-C₁)PhO]₈PcCu (**3b**) shows a monotropic Col_{ro}(P2m) mesophase. Thus, we have revealed that mesomorphism could be induced by these novel bulky substituents instead of using long alkyl chains, and that the mesophase structures were greatly affected by the number and position of methoxy groups. Especially, it is very interesting that the derivatives having methoxy group(s) at the *meta* position(s), **3c**, **3e**, **3f** and **3g**, tend to show enantiotropic mesophase(s), whereas neither the derivative having no methoxy group, **3a**, nor the derivative having a methoxy group at the *para* position, **3d**, show a mesophase.

1 Introduction

Generally, liquid crystalline materials are broadly categorized into rod-like (calamitic) and disk-like (discotic) molecules from their molecular shapes. In addition to the major of calamitic and discotic molecules, banana-shaped, T-shaped and the other shaped molecules are also known as a minor of liquid crystalline materials. Nevertheless, each of the liquid crystals has a flat rigid central core and several flexible long alkyl chains in the periphery in almost all the cases.¹ When the liquid crystals are heated, the peripheral long alkyl chains melt to form soft parts at first, whereas the central cores remain without melting. Generally, it may induce a liquid crystalline phase (= mesophase). Hence, people have long believed an essential requirement that a liquid crystalline molecule should have long alkyl chains in the periphery. Since the discovery of the first liquid crystals in 1888, almost all the liquid crystals consist of a central rigid core and several peripheral long alkyl chains. Up to date, about 101,000 kinds of liquid crystals have been synthesized¹ and investigated in various fields, especially in liquid crystal display.²

However, in 1911 Vorländer found unique liquid crystals having neither a rigid core nor peripheral long alkyl chains.³ They have been forgotten for about 100 years and a very few research on this type of liquid crystals have been done.⁴⁻⁸ Figure 1-(1) shows a representative molecular structure of sodium diphenyl

acetate, Ph₂CHCOONa (**1**). In 2006, we revealed at the first time by using temperature-dependent X-ray diffractometer that this salt, Ph₂CHCOONa (**1**), shows a hexagonal columnar (Col_h) mesophase.⁸ The mesophase structure is also depicted in Figure 1-(1). As can be seen from this figure, the bulky substituent freely rotates around the bond coloured in red ink to form a soft corn-shaped part instead of long alkyl chains to show the columnar mesophase. In this mesophase, sodium metals form a one-dimensional nano-wire and freely rotating diphenyl acetates cover the nano-wire to form an aromatic nanotube. The mesophase-showing mechanism due to free rotation of the bulky substituent very resembles flying seeds of maple, so that we named such unique liquid crystals as “flying-seed-like liquid crystals”.⁸

In 2009, Usol'tseva and her co-workers found from polarizing optical microscopic observations that a phthalocyanine (Pc) derivative substituted by four triphenylmethyl groups, (3Ph-PhO)₄PcCu (**2**), depicted in Figure 1-(2) shows a mesophase.^{9, 10} The substituent of triphenylmethyl group in this compound very resembles the molecular structure of Ph₂CHCOONa (**1**) in Figure 1-(1). Therefore, we thought that this Pc derivative might be one of the flying-seed-like liquid crystals induced by free rotation of the peripheral bulky substituents. In 2012, we carried out temperature-dependent X-ray diffraction studies on this Pc derivative **2** and revealed that it also shows a hexagonal columnar mesophase.¹¹ Furthermore, we recently reported that introduction

of the bulky substituents to the other cores also induce mesomorphism.¹²

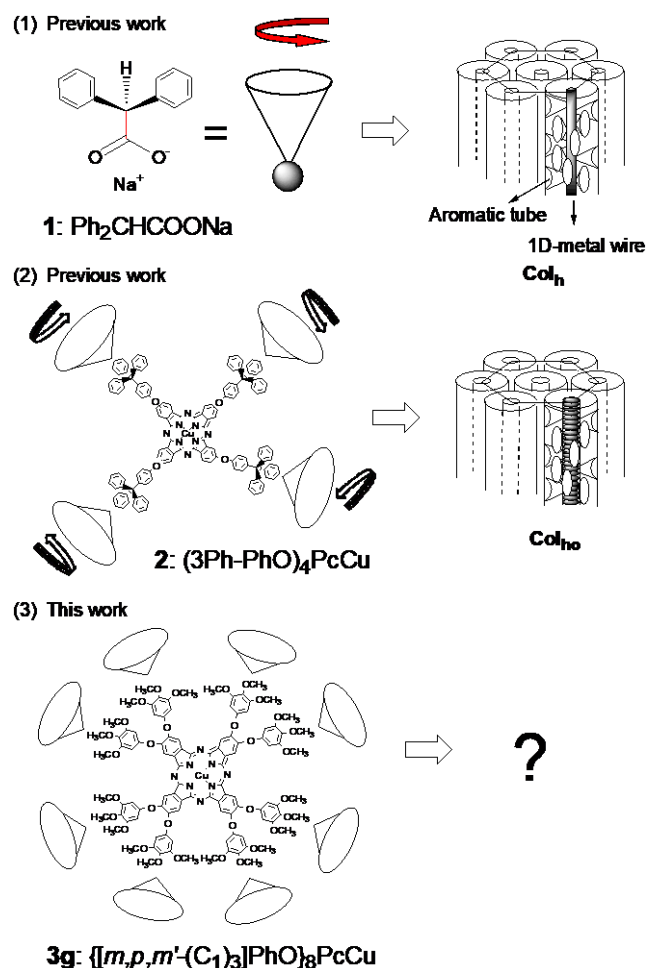


Fig. 1 Molecular and mesophase structures of flying-seed-like liquid crystals. (1) and (2): Rotating bulky substituents induced mesophases in the previous compounds.^{8, 11} (3): Can we induce mesophases by using novel bulky substituents? One of the bulky substituents used in this work is depicted here.

From these investigations, we successfully established two series of bulky substituents, (i) and (ii), inducing flying-seed-like liquid crystals:

- (i) Diphenylmethyl ($\text{Ph}_2\text{-CH-}$), 2-methylethyl ($(\text{CH}_3)_2\text{-CH-}$) and 3-ethylpropyl ($(\text{C}_2\text{H}_5)_2\text{-CH-}$).⁸
- (ii) 4-(Triphenylmethyl)phenoxy (3Ph-PhO-), 4-(1, 1-diphenylethyl)phenoxy (2PhO-PhO-), 4-(1-methyl-1-phenyl)phenoxy (1Ph-PhO-) and 4-(*tert*-butyl)phenoxy (0Ph-PhO-).^{11, 12}

Although a very few other liquid crystals having neither a rigid central core nor flexible peripheral long alkyl chains have been reported until now,¹³⁻¹⁷ the mesophase-originating mechanism has never been clarified without our flying-seed-like liquid crystals.^{8, 12, 13} Accordingly, we have planned to find out a novel series of bulky substituents inducing mesomorphism except (i) and (ii), because we thought that we could further clarify how the compounds having no alkyl chains would show mesomorphism.

The previous bulky substituents of (i) and (ii) freely rotate by

360° . When bulky substituents would rotate not by 360° but flip-flop by restricted angle region, can such bulky substituents induce mesomorphism? For example, in Figure 1-(3) is illustrated $[\text{m},\text{p},\text{m}'\text{-(C}_1)_3\text{]PhO)}_3\text{PcCu}$ (**3g**) substituted by trimethoxyphenoxy groups; can the phthalocyanine derivative show mesomorphism? In this compound, two adjacent phenoxy groups cannot freely rotate but flip-flop within the restricted angles. However, when this phenoxy group is further substituted by three methoxy groups at the *m*, *p*, *m'*-positions, the resulting bulkier substituent, $[\text{m},\text{p},\text{m}'\text{-(C}_1)_3\text{]PhO}$, originates bigger excluded volume by the flip-flop. Accordingly, mesomorphism may be also induced not only by free rotation but also by flip-flop of bulky substituents.

In this study, we have synthesized the PcCu derivatives **3a~g** substituted by a novel series of bulky substituent groups **a~g**:

- (iii) PhO (**a**); (*o*- C_1)PhO (**b**); (*m*- C_1)PhO (**c**); (*p*- C_1)PhO (**d**); $[\text{m},\text{p}\text{-(C}_1)_2\text{]PhO}$ (**e**); $[\text{m},\text{m}'\text{-(C}_1)_2\text{]PhO}$ (**f**); $[\text{m},\text{p},\text{m}'\text{-(C}_1)_3\text{]PhO}$ (**g**),

to investigate their mesomorphism. As a result, we found that the derivatives having methoxy group(s) at the *meta* position(s) tend to show enantiotropic mesophase(s). We wish to report here the interesting results.

2 Experimental Section

2.1 Synthesis

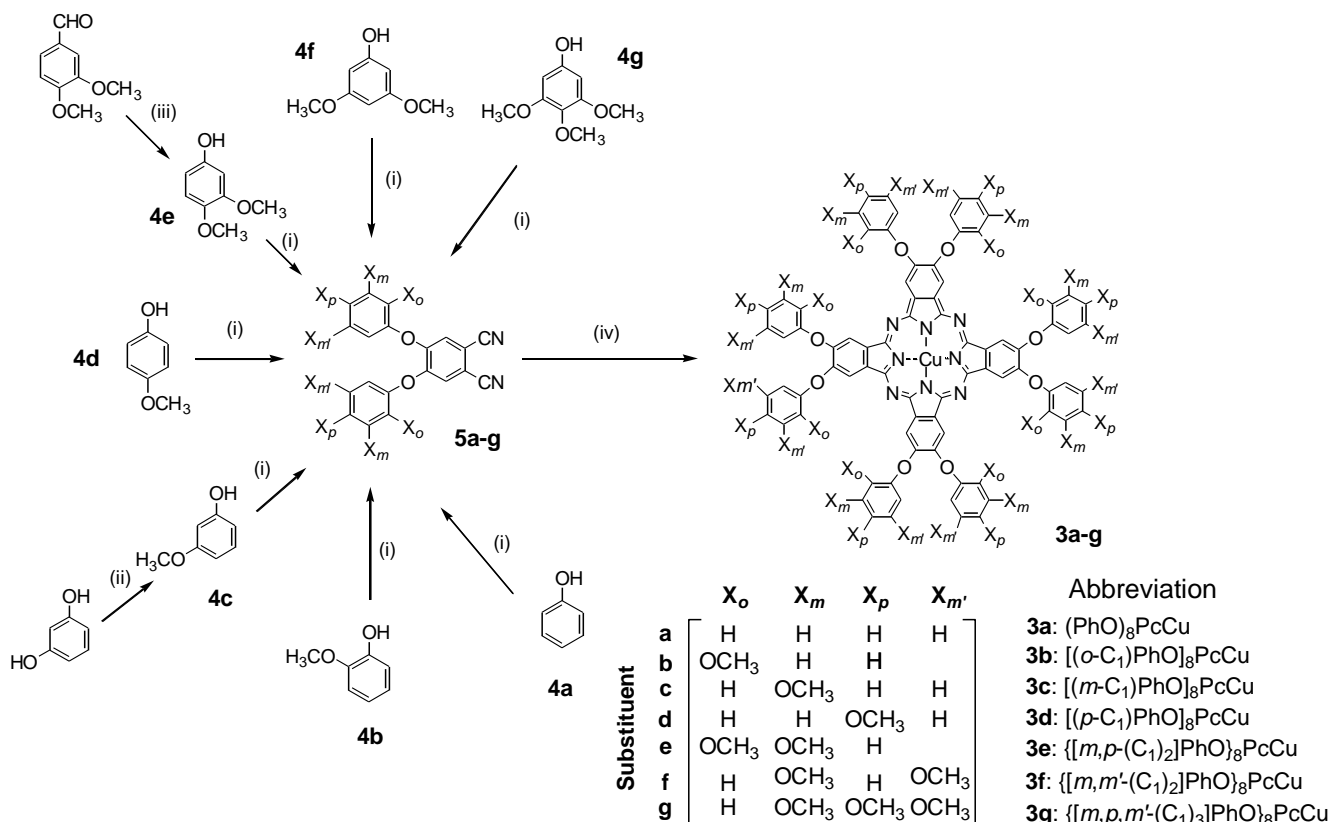
The phthalocyanine derivatives, **3a~g**, were synthesized according to Scheme 1. The precursor of phenol derivative **4c** was synthesized from commercially available resorcinol (Wako) and iodomethane (Wako) by using our previously reported method.¹⁸ The precursor of phenol derivative **4e** was synthesized from commercially available 3, 4-dimethoxybenzaldehyde (Wako) by using our previously reported method.¹⁹ The other phenol derivatives, **4a**, **4b**, **4d**, **4f** and **4g**, were purchased from Tokyo Kasei. These phenol derivatives (**4a~g**) were reacted with commercially available 4, 5-dichlorophthalonitrile (Tokyo Kasei) to obtain the corresponding phthalonitrile derivatives (**5a~g**), which were converted into the corresponding phthalocyanine derivatives (**3a~g**).

The detailed synthetic procedures are described below only for the representative phthalocyanine derivative, $[\text{m}\text{-(C}_1\text{)PhO}]_8\text{PcCu}$ (**3c**). For the other precursors (**5a~b**, and **5d~g**) and phthalocyanine derivatives (**3a~b**, and **3d~g**), the physical property data are only described.

3-Methoxyphenol (**4c**)

A mixture of resorcinol (2.67 g, 24.3 mmol), K_2CO_3 (5.30 g, 38.3 mmol) and dry DMF (30 ml) in a 100 ml of three necked flask was stirred at 110°C under a nitrogen atmosphere for 20 min. Then, iodomethane (7.86 g, 55.4 mmol) was added to the mixture and it was stirred at 110°C under a nitrogen atmosphere for 1.0 h. After cooling to rt, the reaction mixture was extracted with chloroform and washed with water. The organic layer was dried over Na_2SO_4 overnight. After removing the Na_2SO_4 by filtration, the filtrate was evaporated *in vacuo* by using an evaporator. The residue was purified by column chromatography (silica gel, chloroform, $R_f = 0.18$) to obtain 0.882 g of reddish brown liquid. Yield = 29.4%.

$^1\text{H-NMR}$ (CDCl_3 ; TMS) $\delta = 7.13$ (t; J = 9.60 Hz; 1H, Ar-H), 6.49 (d; J = 9.9 Hz; 1H, Ar-H), 6.45-6.39 (m; 2H, Ar-H), 5.67 (s; 1H,



Scheme 1 Synthetic route for novel flying-seed-like phthalocyanines, 3a-g. (i) 4,5-dichlorophthalonitrile, K₂CO₃ and DMA, (ii) CH₃I, K₂CO₃ and DMF, (iii) conc. H₂SO₄, 30% H₂O₂, CHCl₃ and CH₃OH, (iv) CuCl₂, DBU, 1-octanol for **3a**, **3c**, **3d** and **3e**; CuCl₂, DBU and 1-hexanol for **3b**, **3f** and **3g**. DMF = N,N'-dimethylformamide, DMA = N,N'-dimethylacetamide and DBU = 1,8-diazabicyclo[5.4.0]-undec-7-ene.

-OH), 3.77 (s; 1H, -OCH₃).

IR (KBr, cm⁻¹): 3363 (-OH), 2968 (-CH₃), 2842 (-OCH₃).

4,5-Bis(3-methoxyphenoxy)phthalonitrile (**5c**)

In a 100 ml of three necked flask, a mixture of 3-methoxyphenol (**4c**) (0.780 g, 6.28 mmol), K₂CO₃ (6.37 g, 46.1 mmol) and dry DMA (30 ml) was stirred at 110 °C under a nitrogen atmosphere for 15 min. Then, 4,5-dichlorophthalonitrile (0.566 g, 2.87 mmol) was added to the mixture and it was stirred at 110 °C under a nitrogen atmosphere for 3.0 h. After cooling to rt, the reaction mixture was extracted with diethyl ether and washed with water. The organic layer was dried over Na₂SO₄ overnight. After removing Na₂SO₄ by filtration, the filtrate was evaporated *in vacuo* by using an evaporator. The residue was purified by column chromatography (silica gel, dichloromethane, R_f = 0.53) to obtain 0.856 g of white solid. Yield = 80.8%. M.p. = 134 °C.

¹H NMR (CDCl₃; TMS) δ = 7.35 (t; J = 8.08 Hz; 2H, CN-Ar-H), 7.20 (s; 2H, Ar-O-Ar-H), 6.83 (d; J = 8.84 Hz; 2H, Ar-O-Ar-H), 6.66-6.61 (m; 4H, Ar-O-Ar-H), 3.82 (s; 6H, -OCH₃).

IR (KBr, cm⁻¹): 2920 (-CH₃), 2837 (-OCH₃), 2222 (-CN).

4,5-Diphenoxyphthalonitrile (**5a**)

Yield = 78.9%. M.p. = 147.9 °C.

¹H-NMR (CDCl₃; TMS) δ = 7.78(s; 2H, NC-Ar-H), 7.43(t; J = 8.00 Hz; 4H, Ar-O-Ar-H), 7.23(t; J = 8.00 Hz; 2H, Ar-O-Ar-H), 7.10(d; J = 8.00 Hz; 4H, Ar-O-Ar-H).

IR (KBr, cm⁻¹): 2249 (-CN).

4,5-Bis(2-methoxyphenoxy)phthalonitrile (**5b**)

Yield = 92.8%. M.p. = 138.2 °C.

¹H NMR (CDCl₃; TMS) δ = 7.22 (dd; J₁ = 8.08 Hz, J₂ = 7.83 Hz; 2H, NC-Ar-H), 7.10 (d, J = 8.09 Hz; 2H, Ar-O-Ar-H), 6.98 (dd; J₁ = 8.84 Hz, J₂ = 8.08 Hz; 4H, Ar-O-Ar-H), 6.86 (s; 2H, Ar-O-Ar-H), 3.75 (s; 6H, -OCH₃).

IR (KBr, cm⁻¹): 2930, 2820 (-CH₃), 2210 (-CN).

4,5-Bis(4-methoxyphenoxy)phthalonitrile (**5d**)

Yield = 93.4%. M.p. = 158.0 °C.

¹H NMR (CDCl₃; TMS) δ = 6.98 (m; 6H, NC-Ar-H and Ar-O-Ar-H), 6.91 (d, J = 8.84 Hz; 4H, Ar-O-Ar-H), 3.79 (s; 6H, -OCH₃).

IR (KBr, cm⁻¹): 2912(-CH₃), 2233 (-CN).

4,5-Bis(3,4-dimethoxyphenoxy)phthalonitrile (**5e**)

Yield = 13.3%. M.p. = 189 °C.

¹H NMR (CDCl₃; TMS) δ = 7.10 (s; 2H, NC-Ar-H), 6.92 (d; J = 8.84 Hz; 2H, Ar-O-Ar-H), 6.67 (d; J = 9.16 Hz, 4H, Ar-O-Ar-H), 3.93 (s; 6H, -OCH₃), 3.88 (s; 6H, -OCH₃).

IR (KBr, cm⁻¹): 2930, 2836 (-CH₃), 2233 (-CN).

4,5-Bis(3,5-dimethoxyphenoxy)phthalonitrile (**5f**)

Yield = 21.2%. M.p. = 263.4 °C.

¹H NMR (CDCl₃; TMS) δ = 7.12 (s; 2H, NC-Ar-H), 6.30 (t, J = 2.78 Hz; 2H, Ar-O-Ar-H), 6.15 (s; 4H, Ar-O-Ar-H), 3.72 (s; 12H, -OCH₃).

IR (KBr, cm⁻¹): 2923, 2853(-CH₃), 2233 (-CN).

4,5-Bis(3,4,5-trimethoxyphenoxy)phthalonitrile (**5g**)

Yield = 76.8%. M.p. = 230.2 °C.

¹H NMR (CDCl₃; TMS) δ = 7.42 (s; 2H, NC-Ar-H), 6.01-5.92 (m; 4H, Ar-O-Ar-H), 3.71 (s; 18H, -OCH₃).

IR (KBr, cm^{-1}); 2943, 2833(-CH₃), 2233 (-CN).

[(*m*-C₁)PhO]₈PcCu (3c)

In a 50 ml of three necked flask, a mixture of 4,5-bis(3-methoxyphenoxy)phthalonitrile (**5e**) (0.505 g, 1.35 mmol), 1-octanol (5 ml), CuCl₂ (0.103 g, 0.766 mmol) and DBU (4 drops) was refluxed under a nitrogen atmosphere for 17 h. After cooling to rt, the reaction mixture was poured into methanol to precipitate the

target compound. The methanolic layer was removed by filtration and then the resulting precipitate was washed with methanol, ethanol and acetone, respectively. The residue was purified by column chromatography (silica gel, chloroform : THF = 9:1, R_f = 0.70) and recrystallization from ethyl acetate to obtain 0.347 g of green solid. Yield = 66.7%.

15 Table 1 . Yields, MALDI-TOF mass spectral data and elemental analysis data of **3a~g**.

Compound	Yield (%)	Mol. formula (Exact Mass)	Observed Mass	Mol. formula (Average Mass)	Element analysis; found(%) (calculated %)		
					C	H	N
3a: (PhO) ₈ PcCu	48.4	C ₈₀ H ₄₈ N ₈ O ₈ Cu (1311.29)	1311.17	C ₈₀ H ₄₈ N ₈ O ₈ Cu (1312.87)	-	-	-
3b: [(<i>o</i> -C ₁)PhO] ₈ PcCu	65.5	C ₈₈ H ₆₄ N ₈ O ₁₆ Cu (1551.38)	1551.27	C ₈₈ H ₆₄ N ₈ O ₁₆ Cu (1553.04)	68.06 (68.44)	4.49 (4.15)	6.92 (7.22)
3c: [(<i>m</i> -C ₁)PhO] ₈ PcCu	66.7	C ₈₈ H ₆₄ N ₈ O ₁₆ Cu (1551.38)	1551.24	C ₈₈ H ₆₄ N ₈ O ₁₆ Cu (1553.04)	67.76 (68.44)	4.14(4.15)	7.12 (7.22)
3d: [(<i>p</i> -C ₁)PhO] ₈ PcCu	35.6	C ₈₈ H ₆₄ N ₈ O ₁₆ Cu (1551.38)	1551.29	C ₈₈ H ₆₄ N ₈ O ₁₆ Cu (1553.04)	-	-	-
3e: {[<i>m,p</i> -(C ₁) ₂]PhO} ₈ PcCu	39.0	C ₉₆ H ₈₀ N ₈ O ₂₄ Cu (1791.46)	1791.27	C ₉₆ H ₈₀ N ₈ O ₂₄ Cu (1793.29)	-	-	-
3f: {[<i>m,m'</i> -(C ₁) ₂]PhO} ₈ PcCu	53.0	C ₉₆ H ₈₀ N ₈ O ₂₄ Cu (1791.46)	1791.37	C ₉₆ H ₈₀ N ₈ O ₂₄ Cu (1793.29)	-	-	-
3g: {[<i>m,p,m'</i> -(C ₁) ₃]PhO} ₈ PcCu	80.5	C ₁₀₄ H ₉₆ N ₈ O ₃₂ Cu (2031.55)	2031.58	C ₁₀₄ H ₉₆ N ₈ O ₃₂ Cu (2033.46)	61.59 (61.43)	4.46 (4.76)	5.63 (5.51)

-: This compound did not completely burn out so that the observed carbon content showed lower by several percent than the calculated values. Therefore, these elemental analysis data are omitted here.

20 Table 2. Electronic absorption spectral data of **3a~g**.

Compound	Concentration [#] (X10 ⁻⁵ mol/l)	λ_{max} (nm) (log ϵ)						
		Soret-band			Q-band			
3a: (PhO) ₈ PcCu	-	-	-	-	-	-	-	-
3b: [(<i>o</i> -C ₁)PhO] ₈ PcCu	1.03	278.2(4.77)	292.9(4.75)	341.7(4.84)	ca.400(4.43)	613.9(4.58)	651.4(4.54)	682.8(5.33)
3c: [(<i>m</i> -C ₁)PhO] ₈ PcCu	1.03	-	284.2(4.94)	341.7(5.00)	ca.400(4.55)	614.6(4.78)	650.7(4.79)	681.5(5.41)
3d: [(<i>p</i> -C ₁)PhO] ₈ PcCu	-	-	-	-	-	-	-	-
3e: {[<i>m,p</i> -(C ₁) ₂]PhO} ₈ PcCu	0.948	-	291.2(4.86)	340.9(4.88)	ca.420(4.29)	614.6(4.60)	652.6(4.59)	684.3(5.31)
3f: {[<i>m,m'</i> -(C ₁) ₂]PhO} ₈ PcCu	1.00	-	289.2(4.55)	342.2(4.62)	ca.390(4.27)	614.5(4.34)	651.1(4.34)	682.4(4.92)
3g: {[<i>m,p,m'</i> -(C ₁) ₃]PhO} ₈ PcCu	9.84	-	291.6(3.85)	340.4(3.97)	ca.400(4.46)	615.3(3.71)	652.8(4.69)	683.5(5.45)

#: In chloroform. -: This derivative was insoluble in any solvents.

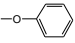
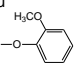
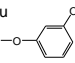
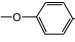
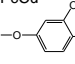
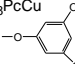
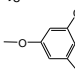
MALDI-TOF Mass data for **3a~g**: See Table 1.
 Elemental Analysis data for **3b, c, g**: See Table 1.
 UV-vis spectral data **3b, c, e~g**: See Table 2.

2.2 Measurements

The compounds synthesized here were identified with a $^1\text{H-NMR}$ spectrometer (BRUKER Ultrashield 400 MHz), a FT-IR spectrometer (Nicolet NEXUS 670), an elemental analyzer (Perkin-Elmer elemental analyzer 2400) and a MALDI-TOF mass spectrometer (AutoflexIII-2S). The elemental analysis data and MALDI-TOF mass spectral data of the phthalocyanine derivatives **3a~g** were summarized in Table 1. Each of the electronic absorption spectra of all the phthalocyanine derivatives was recorded by using a HITACHI U-4100 spectrophotometer

and the data were summarized in Table 2. Phase transition behaviour was observed with a polarizing optical microscope (Nikon ECLIPSE E600 POL) equipped with a Mettler FP82HT hot stage and a Mettler FP-90 central processor, and a Shimadzu DSC-50 differential scanning calorimeter. The decomposition temperatures were measured by a Rigaku Thermo plus TG 820 thermogravimetry analyser. The mesophases were identified by using a small angle X-ray diffractometer (Bruker Mac SAXS System) equipped with a temperature-dependent sample holder to cramp a Mettler FP82HT hot stage (see Figs. S1 and S2 in Ref. 20), which measurable range is from 3.0 Å to 100 Å and the temperature range is from r.t. to 375 °C.²⁰

Table 3. Phase transition temperatures and enthalpy changes of **3a~g**.

Compounds	Phase	T (°C) [ΔH (kJmol ⁻¹)]	Phase	relaxation
3a : (PhO) ₈ PcCu 			K	541 → dc.
3b : [(<i>o</i> -C ₁)PhO] ₈ PcCu 	Glassy Col _{ro} (P2m)	T _g = 87.4	K ₁ → K ₂	177.3[7.20] → 299.4[19.0] → I.L. (1st dc.) → 402 → 2nd dc.
3c : [(<i>m</i> -C ₁)PhO] ₈ PcCu 	Glassy Col _{ro} (P2 ₁ /a)	T _g = 69.9	K → Col _{ro1} (P2 ₁ /a) → Col _{ro2} (P2 ₁ /a) → M _x (1st dc.)	191.3 [13.4] → 255.1[2.69] → 360.1 [10.7] → 405 → 2nd dc.
3d : [(<i>p</i> -C ₁)PhO] ₈ PcCu 			K	363 → dc.
3e : [(<i>m,p</i> -(C ₁) ₂)PhO] ₈ PcCu 			K → Col _{ro} (P2 ₁ /a) → I.L. (1st dc.)	189.0 [21.5] → 351.4 [41.8] → 394 → 2nd dc.
3f : [(<i>m,m'</i> -(C ₁) ₂)PhO] ₈ PcCu 			K → Col _{ro} (C2/m) (1st dc.)	310.5 [14.6] → 430 → 2nd dc.
3g : [(<i>m,p,m'</i> -(C ₁) ₃)PhO] ₈ PcCu 	Glassy Col _{tet,o}	T _g = 67.9	K ₁ → K ₂ → Col _{tet,o} (1st dc.)	157.5 [1.56] → 262.1 [17.1] → 346 → 2nd dc.

Phase nomenclature: K = crystal, Col_{ro} = rectangular ordered columnar mesophase, M_x = unidentified mesophase, Col_{tet,o} = tetragonal ordered columnar mesophase, I.L. = isotropic liquid and dc. = decomposition.

3 Results and Discussion

3.1 Synthesis

In Table 1 are listed the yields, MALDI TOF mass spectral data and elemental analysis data of **3a~g**. As can be seen from this table, each of the mass spectral data of **3a~g** is in good accordance with the calculated exact mass. On the other hand, the elemental analysis data of **3b** and **3g** gave satisfactory values of C, H and N within ±0.4% deviation, but the observed value of C for **3c** is smaller by 0.68% than calculated value and those of H and N are within ±0.4%. Since each of the other derivatives of **3a, 3d, 3e** and **3f** was much less flammable than **3c**, it gave much smaller carbon value by several percent than the calculated value. Therefore, these data are omitted in this table. It is a characteristic for less flammable phthalocyanine derivatives.²¹ Table 2

summarizes the electronic absorption spectral data of **3a~g**. As can be seen from this table, each of the derivatives of **3b, 3c** and **3e~g** gave Q-band and Soret band characteristic to PcCu complex having D_{4h} symmetry. Since the derivatives, **3a** and **3d**, were insoluble in any solvents, no data are listed in this table. However, it could be confirmed from their MALDITOF mass spectra in Table 1 that the target derivatives, **3a** and **3d**, were surely synthesized. Also it could be judged from both the MALDI TOF mass spectra and the electronic absorption spectra of **3e** and **3f** in Tables 1 and 2 that they were surely prepared.

3.2 Phase transition behaviour

Phase transition behaviour of the phthalocyanine derivatives **3a~g** synthesized here is summarized in Table 3. These phase transitions have been established by using a polarizing optical microscope (POM), a differential scanning calorimeter (DSC), a

thermal gravity analyser (TGA) and a temperature-dependent small angle X-ray diffractometer. The phase transition behaviour of all the phthalocyanine derivatives **3a-g** is described in the followings.

As can be seen from Table 3, the (PhO)₈PcCu (**3a**) derivative having no methoxy group showed no mesophase but only a crystalline (K) phase from rt to the decomposition temperature at 541 °C.

As can be seen from Table 3, the [(*o*-C₁)PhO]₈PcCu (**3b**) derivative substituted by a methoxy group at an *ortho*-position in the phenoxy group showed a glassy Col_{ro}(P2m) mesophase from rt for the freshly prepared virgin sample. When it was heated over the glass transition temperature at 87.4 °C, it relaxed to transform into crystalline phase K₁; on further heating, it transformed into another crystalline phase K₂, which decomposed without weight loss (1st decomp.) just after melting at 299.4 °C and then decomposed with weight loss (2nd decomp.) at 402 °C. The two-step decomposition has already found in the other liquid crystals based on phthalocyanine derivatives and studied in detail.²² In this paper, the 1st decomp. was indicated from the absorption spectra that two neighbouring phenyl groups may form a ring by intramolecular ring-closing reaction with losing two hydrogen atoms, which is, therefore, accompanied by almost no weight loss. The 2nd decomp. is a normal thermal decomposition accompanied by a large weight loss.

Figure 2 shows a DSC thermogram on the first heating run of

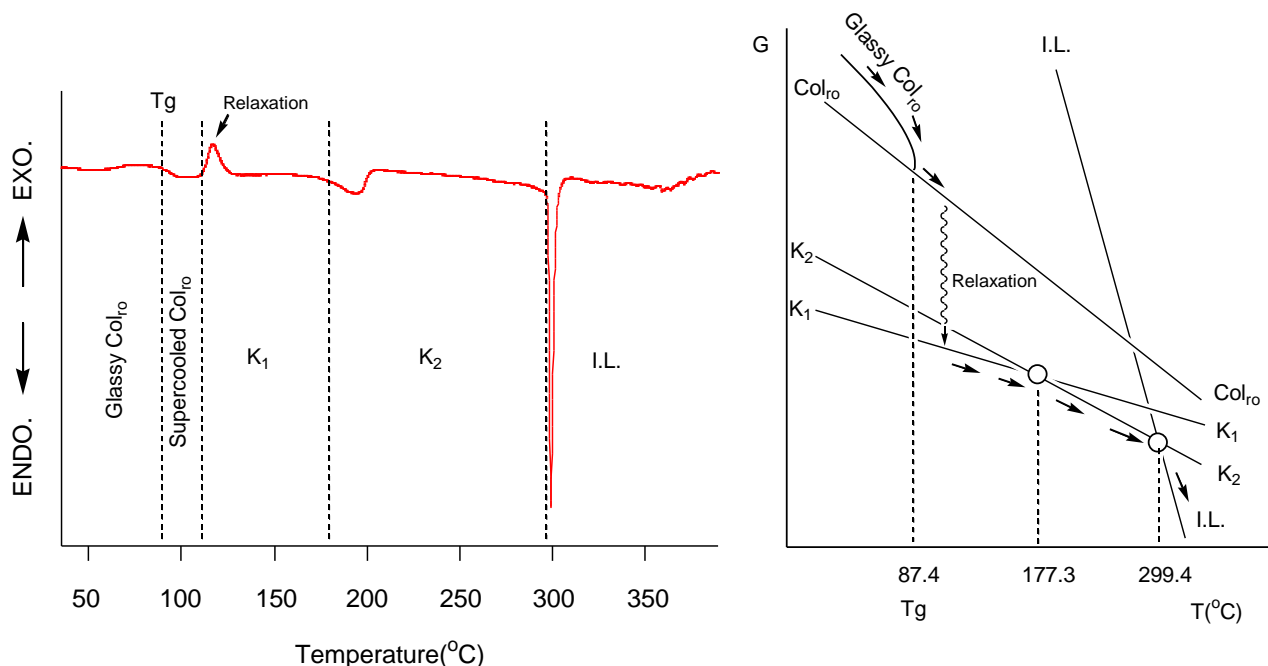


Fig. 2 DSC thermogram and G-T diagram of [(*o*-C₁)PhO]₈PcCu (**3b**) on the 1st heating run.

As can be seen from Table 3, the [(*m*-C₁)PhO]₈PcCu (**3c**) derivative substituted by a methoxy group at a *meta*-position in the phenoxy group also showed a glassy rectangular ordered columnar mesophase Col_{ro}(P2₁/a) at rt for the freshly prepared virgin sample. When it was heated over the glass transition temperature at 69.9 °C, it relaxed into crystalline phase K. On heating, this crystalline phase K transformed into the Col_{ro1}(P2₁/a) mesophase and then another rectangular ordered

[(*o*-C₁)PhO]₈PcCu (**3b**) together with a free energy versus temperature (G-T) diagram. As can be seen from this DSC thermogram, over the glass transition temperature (T_g) at 87.4 °C it shows an exothermic peak at 111.8 °C, which corresponds to the relaxation from supercooled Col_{ro}(P2m) mesophase to crystalline phase K₁;²³ on further heating, it gave a relatively broad endothermic peak at 177.3 °C, which is assigned as a solid-solid (K₁-K₂) phase transition. On heating, it gave a big sharp endothermic peak at 229.4 °C, which is assigned as the melting point, because under microscope, we could observe that the crystals melted into isotropic liquid (I.L.) at this temperature. Such monotropic glassy mesophase transformation behaviour can be rationally explained by using the G-T diagram illustrated in the right part of Figure 2. When the freshly prepared virgin sample was pressed between two glass plates, it was rigid. However, it is crystallographically mesomorphic from the X-ray structural analysis because it has not a 3D lattice but a 2D rectangular lattice having P2m symmetry. Over T_g, it changes into the supercooled Col_{ro} mesophase, in which the more mobile molecules easily rearrange into more stable crystalline phase K₁ by relaxation. It gives an exothermic peak. On heating, K₁ phase transforms into another crystalline phase K₂ by solid-solid phase transition at 177.3 °C. The crystalline phase K² transforms into I.L. at 229.4 °C. These phase transformations occur in order of arrows indicated in this G-T diagram and they can be rationally explained from thermodynamic viewpoint.

columnar mesophase, Col_{ro2}(P2₁/a). On further heating, it transformed into an unidentified mesophase M_x at 360.1 °C, which decomposed without weight loss (1st decomp.) just after the transition and then decomposed with weight loss (2nd decomp.) at 405 °C.

The [(*p*-C₁)PhO]₈PcCu (**3d**) derivative substituted by a methoxy group at a *para*-position in the phenoxy group showed no mesophase but only a crystalline phase (K) from rt to the

decomposition temperature at 363 °C.

The $\{[m,m'-(C_1)_2]PhO\}_8PcCu$ (**3f**) derivative substituted by two methoxy groups at *meta*- and *meta'*- positions in the phenoxy group showed a crystalline phase K from rt, and it melted into a $Col_{ro}(C2/m)$ mesophase at 310.5 °C. It gradually decomposed without weight loss (1st decomp.) over the mp and then decomposed with weight loss (2nd decomp.) at 430 °C.

The $\{[m,p,m'-(C_1)_3]PhO\}_8PcCu$ (**3g**) derivative substituted by three methoxy groups at *meta*-, *para*- and *meta'*- positions in the phenoxy group showed a glassy tetragonal ordered columnar ($Col_{tet,o}$) mesophase at rt. When it was heated over the glass transition temperature (T_g) at 67.9 °C, it relaxed into a crystalline phase K_1 . On further heating, the K_1 phase transformed into another crystalline phase K_2 at 157.5 °C. The K_2 phase melted into the $Col_{tet,o}$ mesophase at 262.1 °C. Over the mp, it gradually decomposed without weight loss (1st decomp.) and decomposed with weight loss (2nd decomp.) at 346 °C.

In our previous work on the long chain-substituted homologues of $(p-C_nOPhO)_8PcCu$, $(m-C_nOPhO)_8PcCu$ and $(o-C_nOPhO)_8PcCu$, we reported that the steric hindrance of a peripheral chain depends on its substitution position and becomes bigger in order of *para* position \rightarrow *meta* position \rightarrow *ortho* position, and that the greater steric hindrance induces weaker interaction among the central Pc cores.²⁴ Compared four present homologous PcCu derivatives **3a-d** with each other, the non-substituted derivative **3a** and the *para*-methoxy-substituted derivative **3d** show only a crystalline phase; the *meta*-methoxy-substituted derivative **3c** only shows enantiotropic mesophases; the *ortho*-methoxy-substituted derivative **3b** only shows isotropic liquid. The PhO group cannot freely rotate due to the neighbouring PhO group, so that the Ph plane twists *ca.* 90° against that of the Pc core. Hence, the angle between the methoxy group and Pc core become smaller in order of *para* position \rightarrow *meta* position \rightarrow *ortho* position. The methoxy group at *meta* position and *ortho* position which stand on the Pc core plane become a steric hindrance to weaken the aggregation (= stacking) of Pc cores. Additionally, the methoxy group at *ortho* position covers the Pc core plane.

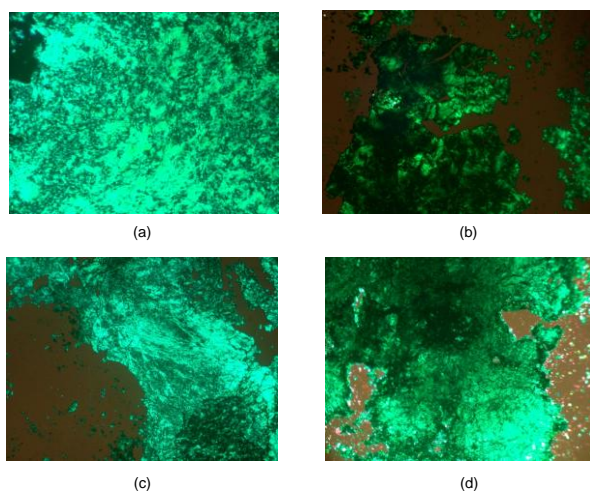


Fig. 3 Photomicrographs of (a) $Col_{ro1}(P2_1/a)$ mesophase of $[(m-C_1)PhO]_8PcCu$ (**3c**) at 230 °C, (b) $Col_{ro}(P2_1/a)$ mesophase of $\{[m,p-(C_1)_2]PhO\}_8PcCu$ (**3e**) at 250 °C, (c) $Col_{ro}(P2_1/a)$ mesophase of $\{[m,m'-(C_1)_2]PhO\}_8PcCu$ (**3f**) at 320 °C, and (d) $Col_{tet,o}$ mesophase of $\{[m,p,m'-(C_1)_3]PhO\}_8PcCu$ (**3g**) at 268 °C.

Therefore, the *meta*-methoxy-substituted derivative **3c** only shows enantiotropic mesophases, and the *ortho*-methoxy-substituted derivative **3b** only shows isotropic liquid.

3.3 Polarizing optical microscopic observation

Figure 3 shows photomicrographs of the Pc derivatives, **3c**, **3e**, **3f** and **3g**, exhibiting mesophases. Figure 3(a)-(d) are the photomicrographs of $[(m-C_1)PhO]_8PcCu$ (**3c**) at 230 °C, $\{[m,p-(C_1)_2]PhO\}_8PcCu$ (**3e**) at 250 °C, $\{[m,m'-(C_1)_2]PhO\}_8PcCu$ (**3f**) at 320 °C, and $\{[m,p,m'-(C_1)_3]PhO\}_8PcCu$ (**3g**) at 268 °C, respectively. Each of these Pc derivatives decomposes without showing isotropic liquid and/or rapidly decomposes just after melting into isotropic liquid, so that it did not show a natural texture which would be obtained by slow cooling from isotropic liquid. However, as can be seen from the photomicrographs in Figure 3, each of the derivatives was spread to show stickiness together with birefringence when the cover glass plate was pressed at the temperature denoted below the photomicrograph. Hence, these states could be identified as mesophases.

3.4 Temperature-dependent X-ray diffraction measurements

In order to clarify the precise mesophase structure, temperature-dependent small angle X-ray diffraction measurements were carried out for the Pc derivatives, **3b**, **3c**, **3e**, **3f** and **3g**, showing mesomorphism. These X-ray diffraction (XRD) patterns and their X-ray data are summarized in Figure 4 and Table 4, respectively. As can be seen from the XRD patterns, no broad halo around $2\theta = 20^\circ$ due to the molten long alkyl chains are observed, although the halo can be generally observed for conventional liquid crystals. It is resulted from no long alkyl chains in the present liquid crystals having only the shortest methoxy groups.

$[(p-C_1)PhO]_8PcCu$ (**3b**)

The $[(p-C_1)PhO]_8PcCu$ (**3b**) derivative substituted by a methoxy group at the *para* position of the phenoxy group shows a glassy mesophase at rt. As can be seen from the XRD pattern in Figure 4[A] and the X-ray data in Table 4, this glassy mesophase gave six reflection peaks. All the peaks except for Peak No. 4 could be well assigned to the reflections from a 2D rectangular lattice having a P2m symmetry and the lattice constants, $a = 20.7 \text{ \AA}$ and $b = 19.2 \text{ \AA}$, by using Reciprocal Lattice Calculation Method.²⁵ Peak No.4 could be assigned to the stacking distance ($h = 7.00 \text{ \AA}$) among the central PcCu cores. Although the stacking distance of 7.00 \AA is very long in comparison with the stacking distances usually observed at $4\sim 5 \text{ \AA}$ for conventional rectangular columnar mesophases, this stacking distance can be proven as a proper value from Z Value Calculation.²⁵

The number (Z) of molecules in a lattice can be calculated from this stacking distance ($h = 7.00 \text{ \AA}$) and the lattice constant of 2D rectangular lattice ($a = 20.7 \text{ \AA}$ $b = 19.2 \text{ \AA}$) listed in Table 4. When ρ , V, N and M are density of mesophase, volume of unite lattice, Avogadro's number and molecular weight, respectively, Z value can be obtained from following equation:

$$\begin{aligned} Z &= (\rho VN)/M = \{\rho [a \times b \times h] N\}/M \\ &= [1.0(\text{g/cm}^3) \times (20.7 \times 10^{-8} \text{ cm}) \times (19.2 \times 10^{-8} \text{ cm}) \times (7.00 \times 10^{-8} \text{ cm}) \times 6.02 \times 10^{23}(\text{mol})]/1553.04(\text{g/mol}) \\ &= 1.08 \\ &\approx 1 \end{aligned}$$

The calculated value $Z \approx 1$ is the same as the theoretical number of molecules in a 2D rectangular lattice having P2m symmetry: Z

= 1.0. Therefore, this big stacking distance $h = 7.00 \text{ \AA}$ is a rationally proper value.

When this glassy $\text{Col}_{\text{ro}}(\text{P2m})$ mesophase was heated over the glass transition temperature at $87.4 \text{ }^\circ\text{C}$, it relaxed into a crystalline phase K_1 . The XRD pattern of K_1 phase gave a lot of sharp peaks in all the regions from low angle to high angle. This apparently

implies that the glassy mesophase crystallized. On heating till the melting point from at $299.4 \text{ }^\circ\text{C}$, no XRD pattern of the $\text{Col}_{\text{ro}}(\text{P2m})$ appeared again. Therefore, the $\text{Col}_{\text{ro}}(\text{P2m})$ mesophase is monotropic and appears only for the freshly prepared virgin sample as a glassy $\text{Col}_{\text{ro}}(\text{P2m})$ mesophase.

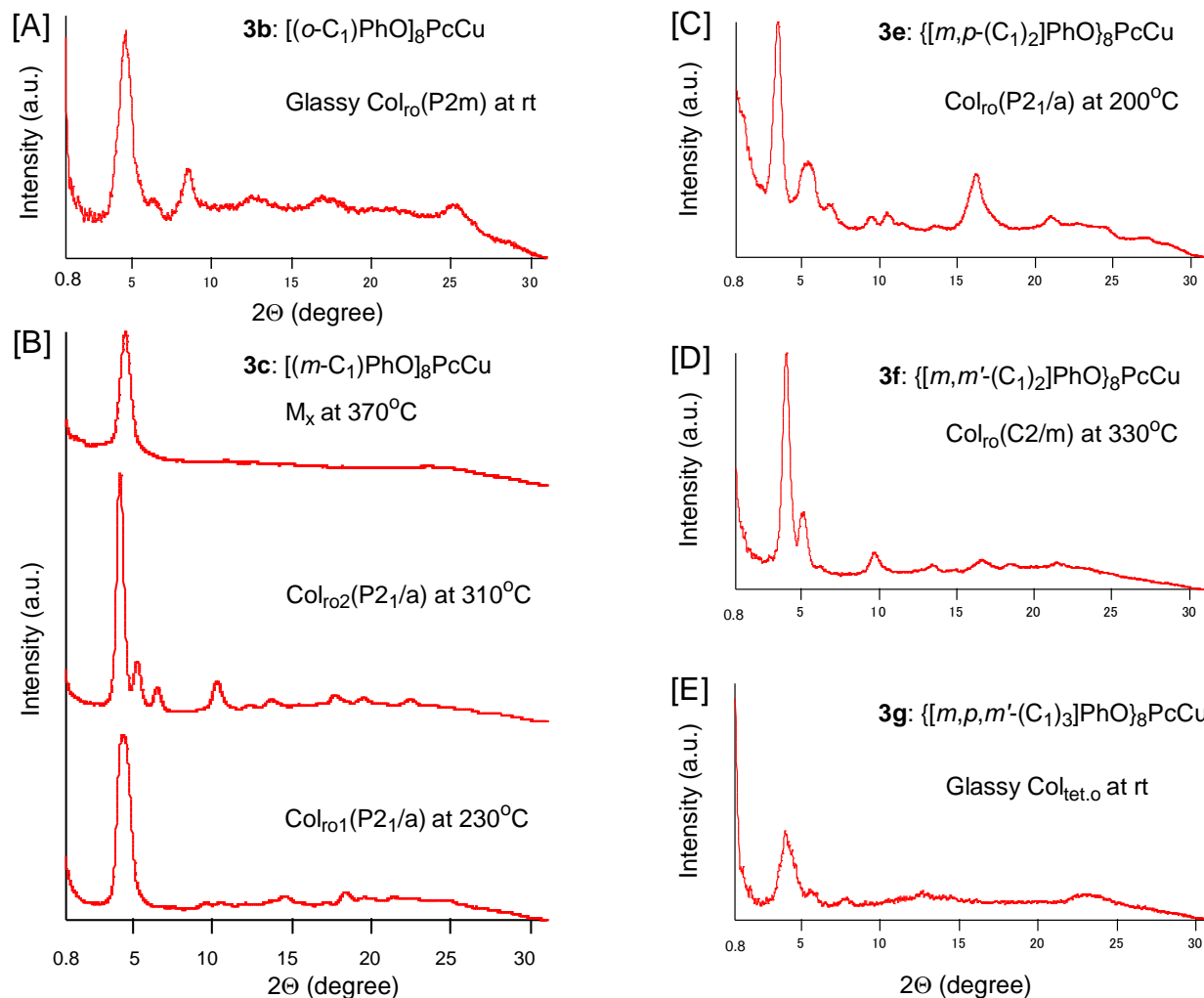


Fig. 4 XRD patterns of the mesophases: [A] $[(o\text{-}C_1)\text{PhO}]_8\text{PcCu}$ (**3b**) at rt; [B] $[(m\text{-}C_1)\text{PhO}]_8\text{PcCu}$ (**3c**) at $230 \text{ }^\circ\text{C}$, $310 \text{ }^\circ\text{C}$ and $370 \text{ }^\circ\text{C}$; [C] $\{[m,p\text{-}(C_1)_2]\text{PhO}\}_8\text{PcCu}$ (**3e**) at $200 \text{ }^\circ\text{C}$; [D] $\{[m,m'\text{-}(C_1)_2]\text{PhO}\}_8\text{PcCu}$ (**3f**) at $330 \text{ }^\circ\text{C}$; [E] $\{[m,p,m'\text{-}(C_1)_3]\text{PhO}\}_8\text{PcCu}$ (**3g**) at rt.

$[(m\text{-}C_1)\text{PhO}]_8\text{PcCu}$ (**3c**)

Figure 4[B] shows the XRD patterns of the $[(m\text{-}C_1)\text{PhO}]_8\text{PcCu}$ (**3c**) derivatives at $230 \text{ }^\circ\text{C}$, $310 \text{ }^\circ\text{C}$ and $370 \text{ }^\circ\text{C}$. As can be seen from the XRD patterns in Figure 4[B] and the X-ray data in Table 4, the XRD pattern at $230 \text{ }^\circ\text{C}$ gave thirteen peaks. All the peaks except for Peak No. 8 could be well assigned to the reflections from a 2D rectangular lattice having a $\text{P2}_1/\text{a}$ symmetry and the lattice constants, $a = 29.4 \text{ \AA}$ and $b = 26.5 \text{ \AA}$. Peak No. 8 could be assigned to the stacking distance ($h = 6.09 \text{ \AA}$). Hence, this mesophase could be identified as a $\text{Col}_{\text{ro}}(\text{P2}_1/\text{a})$ mesophase. The XRD pattern at $310 \text{ }^\circ\text{C}$ gave fifteen peaks. In the same manner described above, this mesophase could be also identified as another $\text{Col}_{\text{ro}}(\text{P2}_1/\text{a})$ mesophase having different lattice constants and stacking distance: $a = 33.6 \text{ \AA}$ and $b = 27.1 \text{ \AA}$, $h = 5.00 \text{ \AA}$. Thus, this derivative exhibited two $\text{Col}_{\text{ro}}(\text{P2}_1/\text{a})$ mesophases having different sets of lattice constants and stacking distance. On

further heating, it showed an unidentified mesophase M_x . As can be seen from the XRD pattern in Figure 4[B] and the X-ray data in Table 4, the M_x mesophase gave only two peaks, so that we could not identify it.

$\{[m,p\text{-}(C_1)_2]\text{PhO}\}_8\text{PcCu}$ (**3e**)

In the same manner described above, the mesophase at $200 \text{ }^\circ\text{C}$ could be identified as a $\text{Col}_{\text{ro}}(\text{P2}_1/\text{a})$ mesophase having lattice constants: $a = 40.2 \text{ \AA}$, $b = 33.1 \text{ \AA}$ and $h = 4.21 \text{ \AA}$.

$\{[m,m'\text{-}(C_1)_2]\text{PhO}\}_8\text{PcCu}$ (**3f**)

In the same manner described above, the mesophase at $330 \text{ }^\circ\text{C}$ could be identified as a $\text{Col}_{\text{ro}}(\text{C2}/\text{m})$ mesophase having a different symmetry $\text{C2}/\text{m}$ with lattice constants: $a = 34.2 \text{ \AA}$ and $b = 28.6 \text{ \AA}$, $h = 4.80 \text{ \AA}$.

$\{[m,p,m'\text{-}(C_1)_3]\text{PhO}\}_8\text{PcCu}$ (**3g**)

The mesophase in this derivative **3g** decomposed so rapidly in the mesomorphic temperature region that the XRD pattern was

measured for the glassy mesophase at rt. As can be seen from Figure 4[E] and Table 4, this glassy mesophase gave five reflections. All the peaks except for Peak No.5 could be assigned to the reflections from a 2D tetragonal lattice having the lattice constant, $a = 22.3 \text{ \AA}$. Peak No. 5 could be assigned to the stacking distance ($h = 3.87 \text{ \AA}$).

Table 4. X-ray data of **3b**, **3c**, **3e**, **3f** and **3g**.

Compound (mesophase)	Mesophase lattice constants(Å)	Peak No.	Spacing(Å)		Miller indices (h k l)
			Obs.	Calc.	
3b : $[(o-C_1)\text{PhO}]_8\text{PcCu}$ (Glassy $\text{Col}_{ro}(\text{P2m})$ at rt)	$a = 20.7$ $b = 19.2$ $h = 7.00$ $Z = 1.1$ for $\rho = 1.0$	1	19.3	19.2	(0 1 0)
		2	13.9	14.1	(1 1 0)
		3	10.4	10.4	(2 0 0)
		4	7.00	-	h
		5	5.15	5.18	(4 0 0)
		6	3.53	3.52	(4 4 0)
3c : $[(m-C_1)\text{PhO}]_8\text{PcCu}$ ($\text{Col}_{ro}(\text{P2}_1/a)$ at 230 °C)	$a = 29.4$ $b = 26.5$ $h = 6.09$ $Z = 2.0$ for $\rho = 1.1$	1	20.1	19.7	(1 1 0)
		2	13.2	13.3	(0 2 0)
		3	11.8	12.1	(1 2 0)
		4	9.24	9.19	(3 1 0)
		5	8.46	8.46	(1 3 0)
		6	7.39	7.35	(4 0 0)
		7	6.51	6.47	(1 4 0)
		8	6.09	-	h
		9	5.17	5.22	(1 5 0)
		10	4.84	4.82	(6 1 0)
		11	4.54	4.60	(6 2 0)
		12	4.41	4.41	(0 6 0)
		13	4.15	4.15	(7 1 0)
3e : $[(m,\rho-C_1)_2\text{PhO}]_8\text{PcCu}$ ($\text{Col}_{ro}(\text{P2}_1/a)$ at 310 °C)	$a = 33.6$ $b = 27.1$ $h = 5.00$ $Z = 2.0$ for $\rho = 1.1$	1	21.1	21.1	(1 1 0)
		2	16.8	16.8	(2 0 0)
		3	13.6	13.6	(0 2 0)
		4	8.61	8.64	(3 2 0)
		5	7.18	7.14	(4 2 0)
		6	6.48	6.52	(5 1 0)
		7	5.73	5.80	(3 4 0)
		8	5.33	5.36	(1 5 0)
		9	5.00	-	h
		10	4.57	4.56	(4 5 0)
		11	4.32	4.32	(6 4 0)
		12	3.97	3.98	(4 6 0)
		13	3.72	3.74	(5 6 0)
		14	3.55	3.55	(8 4 0)
		15	3.42	3.42	(0 8 0)
$(M_x \text{ at } 370 \text{ }^\circ\text{C})$	1	19.5	-	-	
	2	ca. 3.8	-	h	
3f : $[(m,m'-C_1)_2\text{PhO}]_8\text{PcCu}$ ($\text{Col}_{ro}(\text{C2}/m)$ at 330 °C)	$a = 34.2$ $b = 28.6$ $h = 4.80$ $Z = 1.9$ for $\rho = 1.2$	1	21.8	21.9	(1 1 0)
		2	17.3	17.1	(2 0 0)
		3	14.3	14.3	(0 2 0)
		4	9.18	9.18	(1 3 0)
		5	6.56	6.59	(2 4 0)
		6	5.34	5.30	(6 2 0)
		7	4.80	-	h
		8	4.15	4.16	(4 6 0)
3g : $[(m,\rho,m'-C_1)_3\text{PhO}]_8\text{PcCu}$ (Glassy $\text{Col}_{tet,o}$ at r.t. ¹)	$a = 22.3$ $h = 3.87$ $Z = 1.0$ for $\rho = 1.0$	1	22.3	22.3	(1 0 0)
		2	15.9	15.8	(1 1 0)
		3	11.4	11.2	(2 0 0)
		4	7.00	7.07	(3 1 0)
		5	3.87	-	h

h : Stacking distance = (0 0 1), ρ : Assumed density (g/cm^3),

3.5 Mesomorphism depending on the number and position of the methoxy group

Figure 5 illustrates dependence of the mesophase structure on the bulky substituent for the present flying-seed-like liquid crystals based on $(\text{PhO})_8\text{PcCu}$. As can be seen from this figure, the bulkier the substituent becomes, the higher symmetry of mesophase becomes in order of (c, e) \rightarrow f \rightarrow g. Since the bulkiness of the substituent of c and e induced by flip-flop is the same, it may originate the same symmetry of $\text{P2}_1/a$ for **3c** and **3e**.

In Table 5 are summarized the appearance of mesomorphism of the present $(\text{PhO})_8\text{PcCu}$ derivatives **3a**~**g**. As can be seen from this table, the derivatives having methoxy group(s) at the meta position(s), **3c**, **3e**, **3f** and **3g**, show enantiotropic mesophase(s), whereas neither the derivative having no methoxy group, **3a**, nor the derivative having a methoxy group at the para position, **3d**, show a mesophase. The derivative having a methoxy group at

ortho position, **3b**, shows a monotropic mesophase. We discuss about this reason from two points of excluded volume of the phenoxy group originated by flip-flop and steric hindrance of the methoxy group(s) for stacking of the Pc cores.

Figure 6 illustrates three representative molecular structures of $(\text{PhO})_8\text{PcCu}$ (**3a**) showing no mesophase, $[(o-C_1)\text{PhO}]_8\text{PcCu}$ (**3b**) showing a monotropic mesophase, and $[(m-C_1)\text{PhO}]_8\text{PcCu}$

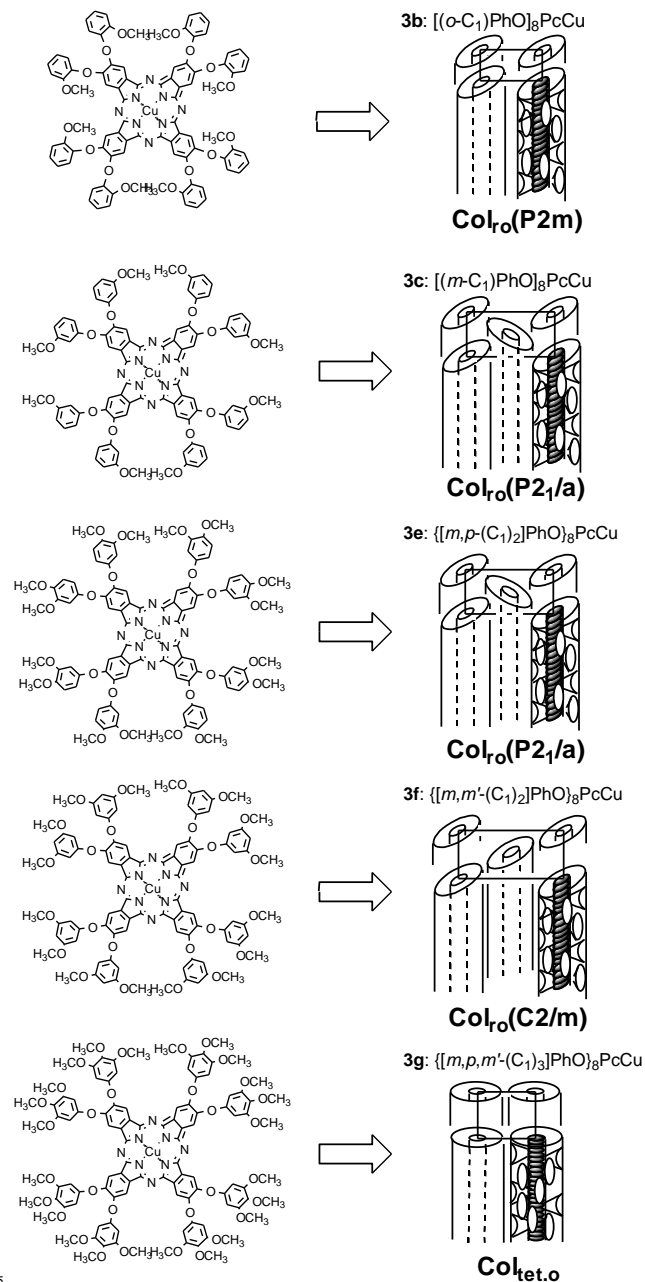


Fig. 5 Dependence of the mesophase structure on the bulky substituent for flying-seed-like liquid crystals based on PhO_8PcCu .

(**3c**) showing an enantiotropic mesophase. In this figure are also schematically illustrated excluded volume originated by the flip-flopping substituent as a corn. As can be seen from this figure, the excluded volume in **3a** showing no mesophase is obviously smaller than the excluded volume in **3c** showing a mesophase. Hence, the excluded volume may be strongly related with the

appearance of mesomorphism: it can be thought that the excluded volume originated by flip-flop of the substituent is too small to form the part soft enough for appearance of a mesophase.

Accordingly, when a methoxy group is substituted at the *para* position in the phenoxy group like as **3d**, the excluded volume is too small to show a mesophase. When a methoxy group is substituted at an *ortho* position like as **3b**, the excluded volume is

Table 5. Appearance of mesomorphism for the flying-seed-like 10 compounds (**3a~g**) based on (PhO)₈PcCu.

Compound	Substituent	X _o	X _m	X _p	X _{m'}	Appearance of mesophase
3a : (PhO) ₈ PcCu		H	H	H	H	×
3b : [(<i>o</i> -C ₁)PhO] ₈ PcCu		OCH ₃	H	H	H	△ (Monotropic)
3c : [(<i>m</i> -C ₁)PhO] ₈ PcCu		H		H	H	○
3d : [(<i>p</i> -C ₁)PhO] ₈ PcCu		H	H	OCH ₃	H	×
3e : {[<i>m,p</i> -(C ₁) ₂]PhO} ₈ PcCu		OCH ₃		H	H	○
3f : {[<i>m,m'</i> -(C ₁) ₂]PhO} ₈ PcCu		H		H	OCH ₃	○
3g : {[<i>m,p,m'</i> -(C ₁) ₃]PhO} ₈ PcCu		H		OCH ₃	OCH ₃	○

×: no mesophase appears; △: monotropic mesophase appears; ○: enantiotropic mesophase appears.

the same as that of **3c**. However, **3c** shows enantiotropic mesophases, whereas **3b** show a monotropic mesophase. It may be attributed to the steric hindrance of the *ortho*-methoxy group that covers the Pc core plane, as already mentioned in the previous session 3-2. The steric hindrance may block the stacking of the central Pc cores to suppress the formation of columnar mesophase. It may decrease the clearing point of mesophase and relatively elevate the melting point of crystalline phase to induce the monotropic mesophase for **3b**.

The driving force of columnar structure formation for disk-like molecules is intermolecular π - π interaction among central cores. It has already reported that peripheral substituents have an effect on the columnar mesophase structures.²⁶⁻²⁸

Since the intermolecular interaction among central cores of a series of the present PcCu-based liquid crystals is also affected by the peripheral bulky substituents, **b**, **c**, **e**, **f** and **g**, the various kinds of columnar mesophases, Col_{ro}(P2m), Col_{ro}(P2₁/a), Col_{ro}(C2/m) and Col_{tet.o}, may be originated. It is very interesting that the appearance of mesomorphism and the mesophase structures are greatly affected by the number and position of the methoxy groups.

4. Conclusion

We have synthesized a novel series of flying-seed-like derivatives

(**3a~g**) based on phthalocyaninato copper(II) (abbreviated as PcCu) substituted by bulky groups {PhO (**a**), (*o*-C₁)PhO (**b**), (*m*-C₁)PhO (**c**), (*p*-C₁)PhO (**d**), [*m,p*-(C₁)₂]PhO (**e**), [*m,m'*-(C₁)₂]PhO (**f**), [*m,p,m'*-(C₁)₃]PhO (**g**)} in order to investigate how they show mesomorphism depending on the number and position of

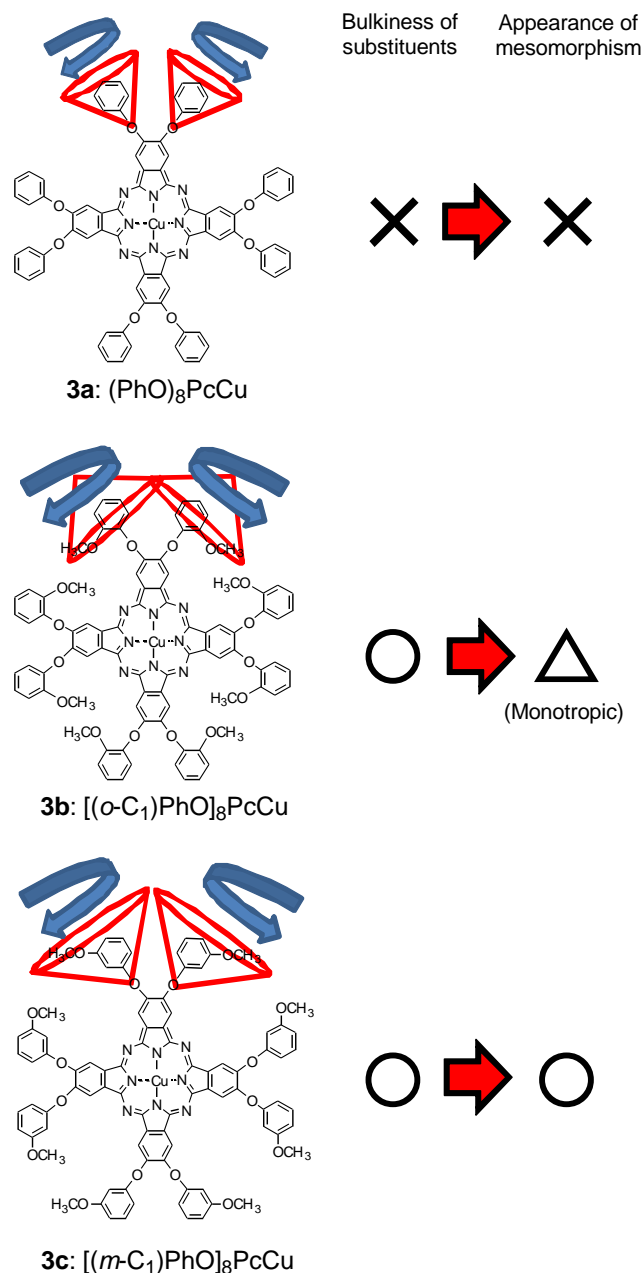


Fig. 6 Appearance of mesomorphism depending on bulkiness of the substituents. ×: no mesophase appears; △: monotropic mesophase appears; ○: enantiotropic mesophase appears.

methoxy groups. As a result, (PhO)₈PcCu (**3a**) and [(*p*-C₁)PhO]₈PcCu (**3d**) show no mesophase, whereas [(*m*-C₁)PhO]₈PcCu (**3c**), {[*m,p*-(C₁)₂]PhO}₈PcCu (**3e**), {[*m,m'*-(C₁)₂]PhO}₈PcCu (**3f**), and {[*m,p,m'*-(C₁)₃]PhO}₈PcCu (**3g**) show various kinds of columnar mesophases of Col_{ro}(P2₁/a), Col_{ro}(P2₁/a), Col_{ro}(C2/m) and Col_{tet.o}, respectively; [(*o*-C₁)PhO]₈PcCu (**3b**) shows a monotropic Col_{ro}(P2m) mesophase.

Thus, the derivative substituted by a methoxy group at a *para* position (**3d**) does not show mesomorphism, because the excluded volume originated by the flip-flopping substituent is small. On the other hand, the derivatives substituted by (a) methoxy group(s) at (a) *meta* position(s) (**3c**, **e**, **f** and **g**) show enantiotropic mesomorphism, because the excluded volume is big enough. The derivative substituted by a methoxy group at an *ortho* position (**3b**) shows monotropic mesomorphism, because the excluded volume is big enough but the steric hindrance may block the stacking the central Pc cores.

In this work, we have revealed that mesomorphism could be induced by these novel bulky substituents instead of using long alkyl chains, and that the mesophase structures were greatly affected by the number and position of methoxy groups. It is very interesting that the derivatives having methoxy group(s) at the *meta* position(s), **3c**, **3e**, **3f** and **3g**, tend to show enantiotropic mesophase(s), whereas neither the derivative having no methoxy group, **3a**, nor the derivative having a methoxy group at the *para* position, **3d**, show a mesophase. We believe that the present examples of novel flying-seed-like liquid crystals will greatly contribute to explore a new field of liquid crystal science.

Notes

^aSmart Material Science and Technology, Interdisciplinary Graduate School of Science and Technology, Shinshu University, 1-15-1 Tokida, Ueda, 386-8567, Japan. E-mail: ko52517@shinshu-u.ac.jp; Fax: +81-268-21-5492; Tel: +81-268-21-5492

^bComprehensive Analysis Center for Science, Saitama University, 255 Shimo-okubo, Sakura-ku, Saitama 338-8570, Japan. E-mail: yasutake@apc.saitama-u.ac.jp; Tel. +81-48-858-3671

^c† Part 3: ref. 12 in this paper.

References

- 1 Database of liquid crystalline compounds for personal computer, LiqCryst Version 5, V. Vill, LCI Publisher and Fujitsu Kyushu Systems Limited, 2010.
- 2 “Handbook of Liquid Crystals, 4 Volume Set”, ed. D. Demus, J. W. Goodby, G. W. Gray, H. W. Spiess and V. Vill, 1998, Wiley-VCH.
- 3 D. Vorländer, *Ber. Dtsch. Chem. Ges.*, 1911, 43, 3120–3125.
- 4 D. Demus, H. Sackmann, and K. Seibert, *Wiss. Z. Univ. Halle, Math.-Nat. R.* 1970, **19**, 47-62.
- 5 P. Ferloni, M. Sanesi, P. L. Tonelli and P. Franzosini, *Z. Naturforsch.* 1978, **33a**, 240-242.
- 6 M. Sanesi, P. Ferloni, G. Spinolo and P. L. Tonelli, *Z. Naturforsch.* 1978, **33a**, 386-388.
- 7 R. van Deun, J. Ramaekers, P. Nockemann, K. van Hecke, L. van Meervelt and K. Binnemans, *Eur. J. Inorg. Chem.*, 2005, 563-571.
- 8 K. Ohta, T. Shibuya and M. Ando, *J. Mater. Chem.*, 2006, **16**, 3635-3639.
- 9 N. Usol'tseva, V. Bykova, G. Ananjeva and N. Zharnikova, *Mol. Cryst. Liq. Cryst.* 20]4, **411**, 1371-1378.
- 10 N. Zharnikova, N. Usol'tseva, E. Kudrik and M. Theakkat, *J. Mater. Chem.*, 2009, **19**, 3161-3167.
- 11 Y. Takagi, K. Ohta, S. Shimosugi, T. Fujii and E. Itoh, *J. Mater. Chem.*, 2012, **22**, 14418-14425.
- 12 A. Hachisuga, M. Yoshioka, K. Ohta, T. Itaya, *J. Mater. Chem.*, 2013, **1**, 5315-5321.
- 13 C. Eaborn and N. H. Hartshorne, *J. Chem. Soc.*, 1955, 549-555.
- 14 J. D. Buning, J. E. Lydon, C. Eaborn, P. M. Jackson, J. W. Goodby and G. W. Gray, *J. Chem. Soc., Faraday Trans.1*, 1982,**78**,713-724.
- 15 S. Basurto, S. Garcia, A. G. Neo, T. Torroba, C. F. Marcos, D. Miguel, J. Barbera, M. B. Ros and M. R. de la Fuente, *Chem. Eur. J.*, 2005, **11**, 5362-5376.

- 16 M. Shimizu, M. Nata, K. Watanabe, T. Hiyama and S. Ujiie, *Mol. Cryst. Liq. Cryst.*, 2005, **441**, 237-241.
- 17 M. Shimizu, M. Nata, K. Mochida, T. Hiyama, S. Ujiie, M. Yoshio and T. Kato, *Angew. Chem. Int. Ed.*, 2007, **46**, 3055-3058.
- 18 H. Sato, K. Igarashi, Y. Yama, M. Ichihara, E. Itoh and K. Ohta, *J. Porphyrins Phthalocyanines*, 2012, **16**, 1148-1181.
- 19 K. Hatsusaka, K. Ohta, I. Yamamoto and H. Shirai, *J. Mater. Chem.*, 2001, **11**, 423-433.
- 20 L. Tauchi, T. Nakagaki, M. Shimizu, E. Itoh, M. Yasutake and K. Ohta, *J. Porphyrins Phthalocyanines*, 2013, **17**, 264-282.
- 21 J. F. van der Pol, E. Neeleman, J. C. van Miltenburg, J. W. Zwikker, R. J. M. Nolte and W. Drenth *Macromolecules*, 1990, **23**, 155–162.
- 22 K. Ohta, T. Watanabe, S. Tanaka, T. Fujimoto and I. Yamamoto, P. Bassoul, N. Kucharczyk and J. Simon, *Liquid Crystals*, 1991, **10**, 357-368.
- 23 M. Sorai and S. Seki, *Bull. Chem. Soc., Jpn.*, 1971, **44**, 2887.
- 24 M. Ichihara, A. Suzuki, K. Hatsusaka and K. Ohta, *J. Porphyrins Phthalocyanines*, 2007, **11**, 503-512.
- 25 K. Ohta, “Dimensionality and Hierarchy of Liquid Crystalline Phases: X-ray Structural Analysis of the Dimensional Assemblies”, Shinshu University Institutional Repository, submitted on 11 May, 2013; <http://hdl.handle.net/10091/17016>; K. Ohta, “Identification of discotic mesophases by X-ray structure analysis,” in “Introduction to Experiments in Liquid Crystal Science (Ekisho Kagaku Jikken Nyumon [in Japanese])”, ed., Japanese Liquid Crystal Society, Chapter 2-(3), pp. 11-21, Sigma Shuppan, Tokyo, 2007; ISBN-13: 978-4915666490.
- 26 P. Herwig, C. W. Kayser, K. Müllen and H. W. Spiess, *Adv. Mater.*, 1996, **8**, 510-513.
- 27 S. Kumar, J. J. Naidu and D. S. S. Rao, *J. Mater. Chem.*, 2002, **12**, 1335-1341.
- 28 R. I. Gearba, M. Lehmann, J. Levin, D. A. Ivanov, M. H. J. Koch, J. Barberá, M. G. Debije, J. Piris and Y. H. Geerts, *Adv. Mater.*, 2003, **15**, 1614-1618.